Journal of Manufacturing Engineering, December 2025, Vol. 20, Issue. 4, pp 159-169
DOI: https://doi.org/10.37255/jme.v20i4pp159-169

ELABORATION AND CHARACTERIZATION OF PVC MATRIX NANOCOMPOSITES REINFORCED WITH NANOCLAY: A CASE STUDY OF MAGHNITE

Bouchareb Badra [1, 2*], Merabet Safia[1, 2], Khouatra Radhia[2], Hamidouche Mohamed[2], Bouchoul Boussaha[2]

[1]Laboratory of Physical and Chemical Properties of High Polymers (LPCHP), Ferhat ABBAS University of Sétif-1, Algeria.
[2]Research Centre in Industrial Technologies CRTI, P.O. Box 64, Cheraga, 16014, Algiers, Algeria.

Abstract

Poly vinyl chloride (PVC)-Maghnite (MMT) nanocomposites were prepared by melt blending using a two-roll mill. The aim of this study was to investigate the effect of incorporating Algerian natural clay (Maghnite), extracted from the Roussel deposit in Maghnia, located in the northwest of Algeria, into the PVC matrix. This nanofiller was incorporated into the PVC matrix at low contents (1 to 4 phr) in two forms: raw (RMMT) and modified (OMMT) using a surfactant (hexadecylamine) and in the presence of a plasticizer (DOP). The properties of PVC-Maghnite nanocomposites were analyzed using multiple physicochemical techniques, including X-ray diffraction (XRD), Fourier-transform infrared spectroscopy (FTIR), thermogravimetric analysis (TGA), Light transmittance, scanning electron microscopy (SEM), and their resistance to degradation was also evaluated. The analyses conducted using XRD and SEM revealed that the modified Maghnite is well dispersed and exfoliated within the PVC matrix. The results obtained from TGA, combined with thermal stability studies and light transmission tests of the various nanocomposites, demonstrate that the incorporation of OMMT enhances the thermal stability of PVC through its barrier effect, which limits the diffusion of heat and volatile decomposition products. Furthermore, the modified Maghnite increases the light transmission (UV, visible, and IR) of the nanocomposites compared to pure PVC and composites containing unmodified Maghnite.

Keywords: *PVC, Raw Maghnite, Modified Maghnite, Nanocomposites, Physical properties*

1. Introduction

The evolution of polymer materials has led to the development of organic matrix composites reinforced with micronic particles, such as talc, fiberglass, or wood chips, known as fillers. The addition of these fillers improves the mechanical and physical properties of the matrix while reducing production costs [1-3]. Over the past decade, there has been a growing interest in a new category of materials reinforced with sub-micronic particles, known as nanocomposites [4]. These particles are characterized by having at least one of their dimensions at the nanoscale. Among the first nanocomposites developed, carbon black-reinforced elastomers have played a significant role, particularly in the tire industry. Today, the economic challenges associated with developing these materials are numerous and impact a wide range of sectors, including construction, automotive, aerospace, electronics, packaging, cosmetics, sports, textiles, and many others [5]. Among the various types of nanocomposites, our study will focus on polyvinyl chloride (PVC)-based nanocomposites, reinforced with lamellar fillers, such as Maghnite. PVC is a widely used thermoplastic polymer, valued for its excellent properties, versatility, and cost-effectiveness, making it a material of choice for many applications [6, 7]. Clay is widely used in the manufacturing of polymer-based composites due to its natural abundance and low cost. It significantly enhances the mechanical, thermal, barrier, and flame-retardant properties of nanocomposites (polymer/clay), without altering their density or reducing their transparency compared to the original materials [8]. Low filler loading rates, ranging from 1 to 5% by weight relative to the base matrix, are sufficient to achieve the desired performance. The hydrophilic nature of lamellar clay presents a compatibility challenge with organic matrices, which are generally hydrophobic. To overcome this incompatibility, surface treatment of the clay is necessary. The most commonly used method is cation exchange, also known as organophilization, which involves the use of surfactants with long carbon chains, with alkylammonium ions being the most widely employed [9].

**Corresponding Author -E-mail: badrabouchareb9@gmail.com*

Journal of Manufacturing Engineering, December 2025, Vol. 20, Issue. 4, pp 159-169
DOI: https://doi.org/10.37255/jme.v20i4pp159-169

The objective of this work is to: Elaborate and characterize nanocomposites based on Poly (Vinyl Chloride) (PVC) reinforced with Maghnite (MMT) type nanofillers (modified or unmodified). For these two samples of Maghnites (MMT), namely Raw Maghnite (RMMT) and Maghnite modified with hexadecylammonium chloride ions (OMMT), are used. Interest was focused in particular on the effect of incorporating these Maghnites at low contents (1, 2, 3, and 4 phr) in the PVC matrix on the properties (structural, thermal, optical, and morphological) of the different nanocomposites (PVC/RMMT and PVC/OMMT).

2. EXPERIMENTAL PROCEDURE

2.1. Materials and Formulations

The polymer used in this study is Poly (Vinyl Chloride) (PVC, 4000 M, K 65–67). It is a product marketed by the National Company of Petrochemical Industries (ENIP) in Skikda (Algeria). It is a thermoplastic polymer with a general formula -$(CH_2$-$CHCl)_n$- generally considered amorphous but can exhibit crystallinity levels in the range of 5-7%. The filler utilized in this study is local clay, known as Maghnite, extracted from the Roussel deposit in Maghnia, located in the northwest region of Algeria (Fig. 1). This clay stands out due to its superior qualities and advantages compared to other types of clay. These include its natural and commercial abundance, low cost, enhanced thermal stability at low concentrations, high resistance to solvents, and its ability to significantly improve the properties of the final blend when used at a low loading (approximately 5% by weight). The chemical composition of Maghnite is as follows: 62.48% SiO_2, 17.53% Al_2O_3, 1.23% Fe_2O_3, 3.59% MgO, 0.82% K_2O, 0.87% CaO, 0.22% TiO_2, 0.39% Na_2O, and 0.04% As [10].

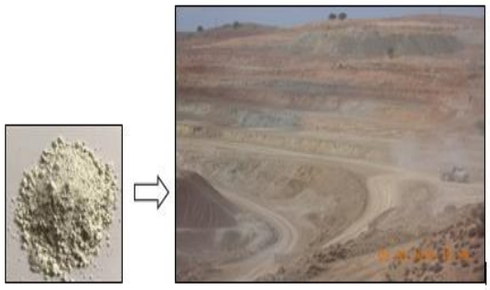

Fig. 1. Presentation of natural Maghnite extracted from the Roussel deposit in Maghnia (Algeria)

2.2. Preparation of the organically-modified Maghnite

A mass of 30 g of raw clay (RMMT) is dispersed in 100 mL of hydrogen peroxide (30%) under stirring for 30 minutes, then diluted to 1 L with distilled water and stirred for 2 hours. After centrifugation, the purified clay is subjected to three successive treatments with a 1 M NaCl solution, followed by washes with distilled water until the absence of chlorides, confirmed by a silver nitrate test. The obtained Maghnite is resuspended, transferred to sedimentation cylinders, decanted, and then centrifuged at 3000 rpm for 35 minutes. It is subsequently dried at 80 °C for 12 hours and sieved to achieve a uniform particle size. This sodium Maghnite is designated by the symbol Na^+MMT. We prepared our modified Maghnite following the protocol of Loïc Le Pluart [11]. 2.41 g of hexadecylamine were dissolved in 1 L of distilled water acidified with 10 mL of hydrochloric acid. The solution was stirred for 3 hours. Then, 5 g of sodium Maghnite (Na^+MMT) were added to the solution, and the mixture was stirred for 6 hours to facilitate the exchange of sodium ions with alkylammonium ions. After centrifugation, the obtained organophilic Maghnite was rinsed several times with hot water (80 °C) to remove inorganic cations. The washing efficiency was verified by a silver nitrate test. The product was then washed with a water/ethanol mixture and filtered. Finally, the Maghnite was vacuum-dried at 85 °C for 36 hours, ground, sieved, and designated as OMMT.

2.3. Processing

Calcium/zinc stearates, DOP, and stearic acid were used as thermal stabilizers, plasticizers, and lubricants, respectively. The composition of the different formulations, which contain PVC, calcium/zinc stearates, DOP, and stearic acid, is presented in Table 1.

Fig. 2. Elaboration of PVC/MMT Nanocomposites Using a Twin-roll Mixer

Journal of Manufacturing Engineering, December 2025, Vol. 20, Issue. 4, pp 159-169
DOI: https://doi.org/10.37255/jme.v20i4pp159-169

The samples (polymer and additives) were prepared by mixing on a two-cylinder mixer (Fig. 2) at a temperature of 160°C. Films of (0.5 ± 0.1) mm thickness are taken after 10 min. The formulations produced are given in the Table 1.

Table 1. The different formulations produced

Formulations	PVC	Stearic arid	Ca/Zn Stearate	Dioctyl phtalate	RMMT (phr)	OMMT (phr)
PVC	100	1	1/1	30	0	0
PVC/RMMT	100	1	1/1	30	1	0
	100	1	1/1	30	2	0
	100	1	1/1	30	3	0
	100	1	1/1	30	4	0
	100	1	1/1	30	5	0
PVC/OMMT	100	1	1/1	30	0	1
	100	1	1/1	30	0	2
	100	1	1/1	30	0	3
	100	1	1/1	30	0	4
	100	1	1/1	30	0	5

phr, parts by weight per hundred parts of resin.

3. MICROSTRUCTURE CHARACTERIZATION

3.1. X-ray diffraction (XRD)

The modification of Maghnite (MMT) and the degree of intercalation of this nanoclay in polymer/nanoclay nanocomposites were studied using X-ray diffraction (XRD). The analyses were performed with a Remake Miniflex diffractometer (UK) equipped with a Cu Kα radiation source. Data were collected at a scanning speed of 1°/min over an angular range of 2° to 30° (2θ).

3.2. FTIR studies

The FTIR spectra of PVC powder, Maghnite powders (modified or unmodified), and nanocomposites were recorded using a PERKIN ELMER 1000 infrared spectrophotometer. The analyses were performed over a wavenumber range from 4000 cm^{-1} to 400 cm^{-1}, with a resolution of 2 cm^{-1} and a fixed number of 10 scans. Nanocomposite films were prepared by compression using a manual Controllable press at a temperature of 160 °C for 3 minutes. The nanofillers were analyzed in the form of pellets obtained by mixing the Maghnite samples with potassium bromide (KBr) at a 2:98 ratio.

3.3. Thermal degradation

The thermal degradation of nanocomposite films (PVC/MMT) was studied at 160°C in an oven. The rectangular films (35 x 25 mm) were placed on an aluminum tray. Samples were taken at six intervals of 10 minutes to monitor the progression of thermal degradation. For each type of nanocomposite (PVC/RMMT and PVC/OMMT), samples degraded at different times were prepared and compared.

3.4. Thermogravimetric Analysis (TGA)

Thermal stability was assessed using an SDTQ 600 thermogravimetric analyzer provided by TA Instruments. Samples ranged from 10 to 15 mg and were subjected to heating under a nitrogen flow (40 mL/min) from room temperature to 700°C, with a heating rate of 10°C/min.

3.5. Light transmittance

The light transmission through PVC/MMT nanocomposite films was measured using a SHIMADZU UV-1800 spectrophotometer (Japan). The samples, square-shaped with dimensions of 2.5 x 2.5 cm^2 and a thickness of 0.5 ± 0.1 mm, were carefully prepared to ensure flat and parallel surfaces, free from dust and internal voids. Measurements were taken in the wavelength range of 200 to 1100 nm with a resolution of 1 nm. The transmission percentages were automatically calculated using the UV Probe software.

3.6 Scanning Electron Microscopy (SEM)

The compatibility among different polymers, as well as the morphological features of the composites, was studied using a scanning electron microscope (JEOL JSM-6390LV) at an accelerating voltage of 5-10 kV. Fractured surfaces of the samples, deposited on a brass holder and sputtered with platinum, were used for this study.

4. RESULTS AND DISCUSSION

4.1. XRD results

4.1.1 X-ray Diffraction (XRD) Analysis of Maghnite

The XRD patterns of powder RMMT (Raw Maghnite) and OMMT (Organically Modified Maghnite) are shown in Fig. 3. The comparison between the two x-

Journal of Manufacturing Engineering, December 2025, Vol. 20, Issue. 4, pp 159-169
DOI: https://doi.org/10.37255/jme.v20i4pp159-169

ray diffractograms (a) and (b) reveals: A peak located at 2θ = 26.59° is indicative of quartz, while the two peaks located at 2θ = 21.88° and 34.77° are attributed to the presence of another impurity [10, 12, 13]. The elimination of impurities in Maghnite generates a narrowing of the characteristic lines of Maghnite [14].

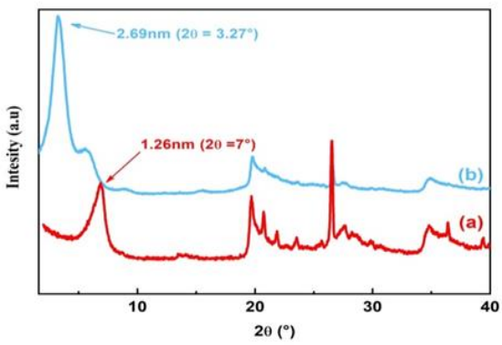

Fig. 3. X-ray diffraction of (a) Raw Maghnite (RMMT) and (b) Organically modified Maghnite by hexadecylammonium chloride ions

The interlayer spacing (d-spacing) of unmodified Maghnite is 1.26 nm, which corresponds to a 2θ value of 7°. Upon modification of Maghnite with hexadecylamine chloride, the interlayer spacing increases to 2.69 nm, corresponding to a 2θ value of 3.27°. This increase in interlayer spacing indicates that hexadecylammonium chloride ions have been intercalated between the layers of Maghnite through a simple cation exchange process (Fig. 4). This modification reaction can be represented as follows:

Reaction 1 corresponds to an electrophilic substitution of the sodium ion (Na^+) by an alkylammonium ion ($R\text{-}NH_3^+$), accompanied by the formation of sodium chloride (NaCl).

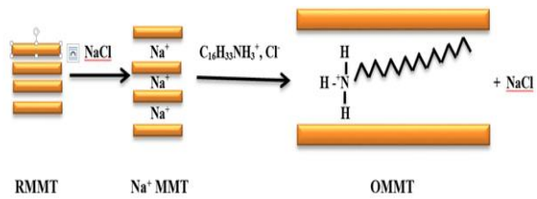

Fig. 4. Schematic representation of the intercalation of the surfactant into the galleries of Maghnite

4.1.2. X-ray Diffraction (XRD) analysis of nanocomposites

Fig. 5 shows the XRD patterns of an unfilled PVC film (0 phr MMT) and PVC/RMMT nanocomposites with various RMMT contents (1, 2, 3, and 4 phr). The results indicate that the (001) peak, characteristic of unmodified Maghnite, appears in the PVC/RMMT nanocomposites at the same angular position as in raw Maghnite alone (see Fig. 3) when 1, 2, and 3 phr of RMMT are incorporated into the PVC matrix. This suggests that the raw Maghnite is simply dispersed in the PVC matrix without any insertion of PVC chains into the interlayer spaces of the RMMT (formation of conventional micro composites). Conversely, the appearance of a new (001) peak in the PVC/RMMT nanocomposites upon incorporating 4 phr of RMMT into the PVC matrix is observed, suggesting the presence of additional RMMT particles not inserted between the macromolecular chains of PVC (agglomeration of RMMT nanoparticles).

On the other hand, Fig. 6 illustrates the diffraction patterns of PVC/OMMT nanocomposites containing 1, 2, 3, and 4 phr of OMMT, respectively. The results show that the addition of OMMT to the PVC matrix leads to increased separation of the interlayer spaces of the OMMT. This is evidenced by the complete disappearance of the (001) peak, characteristic of OMMT, in the range of 1.5 to 40° when 1 to 4 phr of OMMT are incorporated. The absence of (001) diffraction peaks, associated with organophilic Maghnite, suggests that the modified Maghnite layers are clearly separated and exfoliated between the macromolecular chains of PVC [14, 15]. This observation can be attributed to a strong interaction between the polar PVC molecules and the Maghnite layers, resulting in the exfoliation of the OMMT layers.

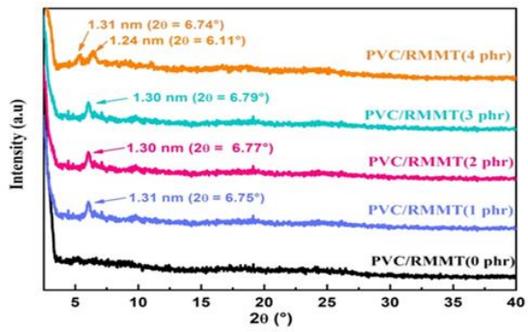

Fig. 5. X-ray diffraction patterns of PVC/RMMT nanocomposites with different contents of RMMT

Journal of Manufacturing Engineering, December 2025, Vol. 20, Issue. 4, pp 159-169
DOI: https://doi.org/10.37255/jme.v20i4pp159-169

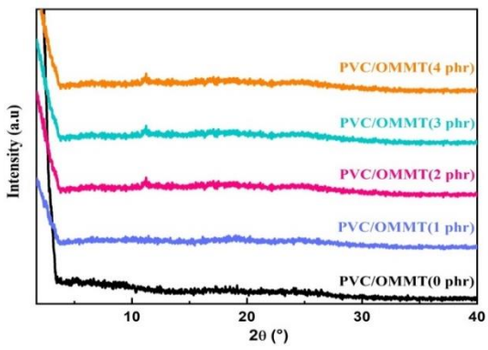

Fig. 6. X-ray diffraction patterns of PVC/OMMT nanocomposites with different contents of OMMT

4.2. FTIR Analysis

The analysis by FTIR spectroscopy was performed to confirm the organophilic modification of Maghnite and to identify the characteristic bands of Maghnite in the different elaborated nanocomposites. Figure 7 shows the FTIR spectra of unmodified Maghnite (curve a) and Maghnite modified by hexadecylamine chloride ions (curve b). The observations are as follows: In the hydroxyl region, extending between 3700 and 3200 cm^{-1}, two bands centered at 3636 and 3416 cm^{-1} are attributed to the stretching vibrations of the O-H bond in the Al-OH and Si-OH groups, as well as absorbed water]16, 17]. A band at 1640 cm^{-1} corresponds to the bending vibrations of the O-H group of water [16-19]. Additionally, a broad band detected around 1089 cm^{-1} is due to the stretching vibrations of the Si-O group in the clay network [20]. The Maghnite modified with hexadecylamine chloride ions show three additional bands around 2990, 2980 and 2830 cm^{-1}, attributed to the valence vibrations of the O-H bond of the methyl and methylene groups present in the surfactant. The bands positioned at 1660, 1550 and 1480 cm^{-1} are attributed to symmetric and asymmetric deformation vibrations of the ammonium group (NH3+) [20]. The low intensity observations located at 3300 and 3030 cm^{-1} are attributed to stretching vibrations of the C-N bond in ammonium. Finally, the weak band at 1250 cm^{-1} is due to the deformation vibrations of the C-N bond of the primary amine [17]. For the PVC/OMMT nanocomposites, a strong absorption band at 1725 cm^{-1} is observed in the FTIR spectra of the unloaded PVC films (0 phr of MMT) as well as in all PVC/RMMT and PVC/OMMT nanocomposites containing 1, 2, 3, and 4 phr of MMT in the PVC matrix. This band is attributed to the elongation vibration of the carbonyl groups (C=O) [21, 22]. In contrast, the FTIR spectrum of PVC powder does not show this vibrational band (see Figure 10), which is explained by the addition of organotin stabilizers in the prepared formulations [21, 23]. The FTIR spectra of the nanocomposites reveal a strong absorption band at 1725 cm^{-1}, present in both unfilled PVC films and all nanocomposites (PVC/RMMT and PVC/OMMT) containing 1, 2, 3, and 4 phr MMT. This band corresponds to the stretching vibration of carbonyl groups (C=O). In contrast, the FTIR spectrum of PVC powder lacks this band (Figure 10), likely due to the addition of organotin stabilizers in the prepared formulations [21, 23]. Furthermore, the unloaded PVC film and all developed nanocomposites show a slight shoulder at 1667 cm^{-1}. This peak is associated with the elongation vibrations of the double bond (C=C), indicating the formation of double bonds in all the prepared nanocomposites [21, 22, 24-27].

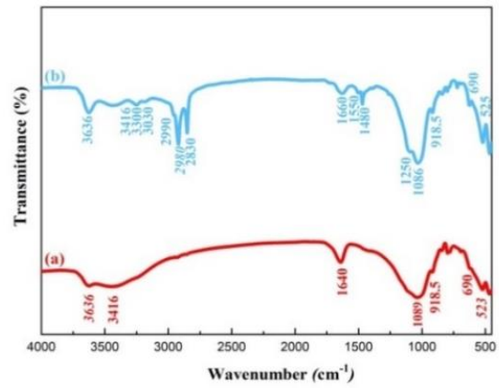

Fig. 7. FTIR Spectra of (a) Raw Maghnite (RMMT) and (b) organically modified Maghnite by hexadecylammonium chloride ions (OMMT)

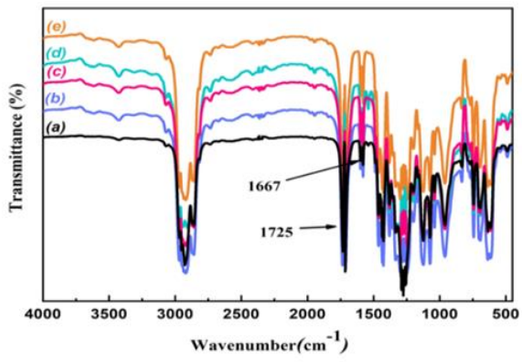

Fig. 8. FTIR spectra of PVC/RMMT nanocomposites with different contents of RMMT

Journal of Manufacturing Engineering, December 2025, Vol. 20, Issue. 4, pp 159-169
DOI: https://doi.org/10.37255/jme.v20i4pp159-169

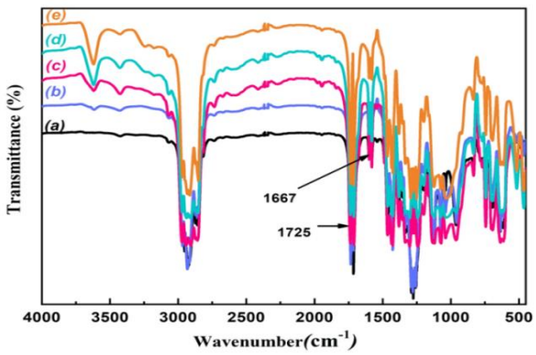

Fig. 9. FTIR spectra of PVC/OMMT nanocomposites with different contents of OMMT

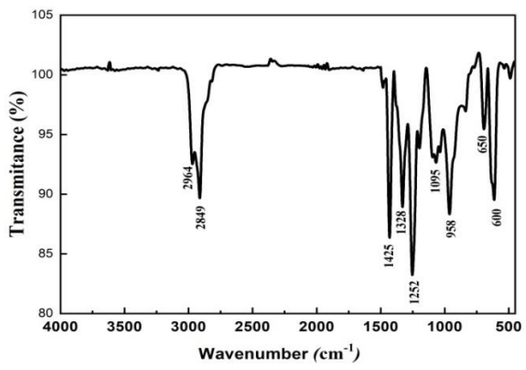

Fig. 10. FTIR spectrum of PVC powder

4.3. Thermal Degradation Study

The study of thermal degradation was carried out due to the importance of the results obtained for PVC samples [28, 29]. To monitor the thermal degradation of nanocomposite samples (PVC/RMMT) and (PVC/OMMT) containing different contents of nanofiller (1, 2, 3, and 4 phr), these samples were subjected to heat treatment at 170°C in an electric oven. The samples, measuring 30 x 25 mm², were placed in the oven and removed after predefined periods. Thus, for each type of nanocomposite (PVC/RMMT) or (PVC/OMMT), a series of thermally degraded samples at different time intervals was prepared. The study of the thermal stability of these nanocomposites was conducted by observing color changes in the samples, following an approach similar to that employed by Peprinicek and co-workers [30]. These samples were then compared using Fig. 11 and 12.

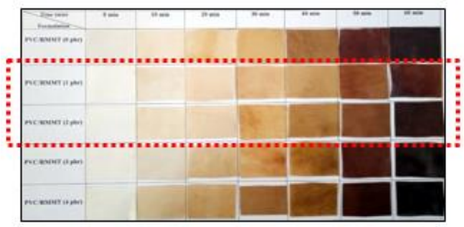

Fig. 11. Change in color of PVC/RMMT nanocomposite samples over time

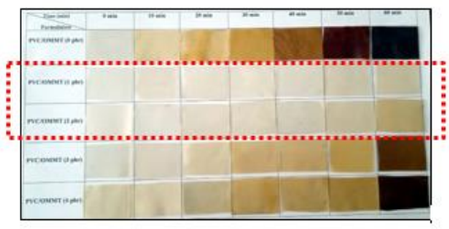

Fig. 12. Change in color of PVC/OMMT nanocomposite samples over time

The thermal stability tests of PVC/RMMT nanocomposites with different RMMT contents show that after 60 minutes of heat treatment, the color change in the samples is similar to that of pure PVC. This indicates that the addition of unmodified Maghnite has no impact on the thermal stability of PVC. Additionally, the first dark color change occurs after 60 minutes, both in pure PVC and in PVC/RMMT nanocomposites. According to Fig. 11, it is observed that when the content of modified Maghnite (OMMT) varies from 1 to 3 phr and samples are taken at 10, 20, 30, 40, 50, and 60 minutes, the color of the PVC/OMMT nanocomposite samples changes from light pink to brown. However, a dark coloration appears when the OMMT content increases significantly (4 phr). These observations suggest that the modification of Maghnite by the alkylammonium present in the interlayer space of the modified Maghnite, which is less thermally stable, is responsible for the coloration of the different PVC/OMMT. These results are similar to those obtained by Peprnicek et al. [30], wan et al. [31], and have also been confirmed by our FTIR analysis. We can conclude that the incorporation of modified Maghnite into the PVC matrix improves the thermal stability of samples at low contents (1, 2, and 3 phr of OMMT). However, at high incorporation rates (4 phr), the PVC/OMMT nanocomposites degrade under heat, leading to the release of hydrochloric acid (dehydrochlorination of

Journal of Manufacturing Engineering, December 2025, Vol. 20, Issue. 4, pp 159-169
DOI: https://doi.org/10.37255/jme.v20i4pp159-169

PVC). Additionally, the decomposition of the intercalated cation also catalyzes the release of HCl (Hoffman degradation) [22]. These processes can be illustrated by the following two reactions:

$$[\text{-CH2-CHCl-}]_n \xrightarrow{\Delta} [\text{-CH=CH-}]_m + [\text{-CH2-CHCl-}]_{n-m} + n\text{HCl}\ \textbf{(Dehydrochlorination of PVC)}\quad (2)$$

$$(C_7H_{15})_2(CH_3)_2N^+, Cl^- \xrightarrow{\Delta} C_5H_{11}\text{-}CH{=}CH_2 + C_7H_{15}(CH_3)_2N + n\text{HCl}\ \textbf{(Hoffman degradation)}\quad (3)$$

4.4 Thermal Gravimetric Analysis (TGA)

Fig. 13 and 14 illustrate the ATG and DTG curves of an unfilled PVC film (0 phr of MMT) and films loaded with various concentrations (1, 2, 3, and 4 phr) of unmodified Maghnite (RMMT) and Maghnite modified with hexadecylammonium chloride ions (OMMT). The thermogravimetric analysis (TGA) results reveal that the unfilled PVC film and all the nanocomposites decompose in two degradation stages [20, 32]. The first stage, occurring in the temperature range of 175 to 350 °C, is characterized by a significant weight loss in all samples, attributed to the dehydrochlorination of PVC (release of hydrogen chloride (HCl) molecules and formation of conjugated polyene sequences) [33]. The second stage occurs at temperatures above 400 °C and corresponds to the cross-linking of chains containing C=C bonds. This thermal degradation process of polyene involves the cyclization and chain scission [34, 35].

Table 2 summarizes the results of the thermogravimetric analysis (TGA) of the different nanocomposites at the first and second stages of degradation. The thermal characteristics studied included the temperature at 1% weight loss (T onset), which is the temperature at the beginning of degradation, the maximum degradation temperatures (T1 max and T2 max), which are the temperatures of maximum thermal degradation obtained from the DTG peaks in the first and second stages, respectively. The maximum degradation rates are designated as V1 max and V2 max, the temperature at 50% mass loss (T 50%), and the residue (R), which is the remaining mass at the end of the test set at 600 °C. Based on the results in Table 2, the thermograms (TGA) of the PVC/OMMT nanocomposites reveal that incorporating different amounts of modified Maghnite (OMMT) into PVC-based formulations significantly improved the thermal stability of these nanocomposites compared to unfilled PVC and PVC/RMMT nanocomposites. These results indicate that the nanoscale dispersion of OMMT fillers at low concentrations can act as a barrier by limiting the diffusion of heat and volatile decomposition products. Consequently, this leads to a significant improvement in the thermal stability of these nanocomposites [31].

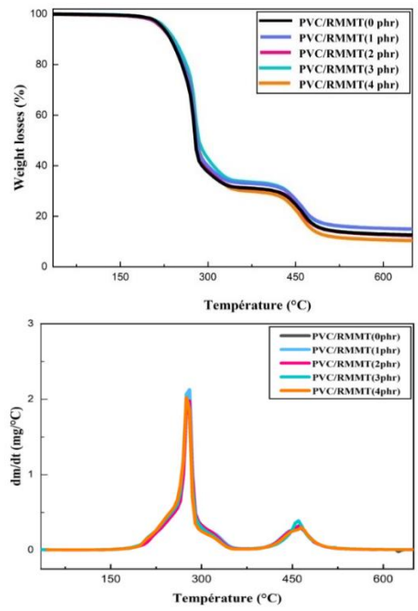

Fig. 13. Analysis by TGA of nanocomposites (PVC/RMMT) with different contents of RMMT

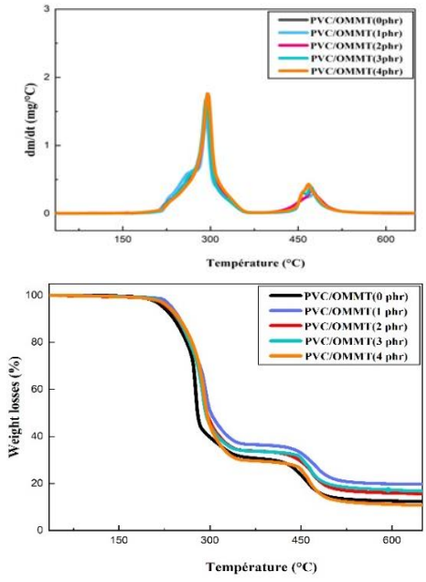

Fig. 14. Analysis by TGA of nanocomposites (PVC/OMMT) with different contents of OMMT

Journal of Manufacturing Engineering, December 2025, Vol. 20, Issue. 4, pp 159-169
DOI: https://doi.org/10.37255/jme.v20i4pp159-169

4.5. Light transmittance

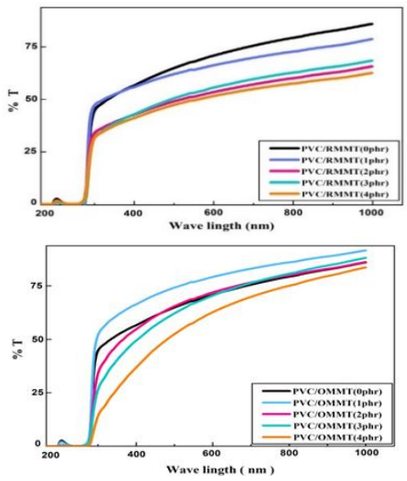

Fig. 15. Variation in light transmission of PVC film and nanocomposites: (a) PVC/RMMT and (b) PVC/OMMT as a function of wavelength

Light transmission (%) involves analyzing the diffusion of electromagnetic radiation through nanocomposite films over various parts of the spectrum: ultraviolet (200-400 nm), visible (400-750 nm), and infrared (750-1000 nm). To facilitate comparison of the developed nanocomposites, representative wavelengths were selected near the middle of each range. Specifically, the transmissions were measured at 300 nm for UV, 550 nm for the visible range, and 900 nm for IR [33]. Fig. 15 illustrates the variation in light transmission (%) of the nanocomposites (PVC/RMMT and PVC/OMMT) as a function of wavelength, while Table 3 summarizes the test results. PVC is an optically transparent polymer in the visible range [33,36,37].

The results of our study clearly show that the light transmission through an unfilled PVC film exceeds 70% in the visible range (Table 3). On the other hand, the incorporation of 1 phr of organophilic Maghnite into the PVC-based formulation results in a significant improvement in the light transmission of the nanocomposite (PVC/OMMT), with respective increases of 54.83%, 78.43%, and 98.53% in the three transmissions ranges: ultraviolet, visible, and infrared, compared to the unfilled PVC film. This improvement is attributed to the homogeneous and uniform dispersion of the modified Maghnite within the PVC matrix. An increase in light transmission is observed below 300 nm (at 240 nm) for all nanocomposites. This transmission band is associated with the C-Cl bond in PVC [37, 38].

Table 2: Thermal gravimetric analysis (TGA) results of the realized formulations

Formulation number	First stage					Second stage			Residue (%) at 600°C
	T Onset (°C)	T^1 max (°C)	V^1 max (%/°C)	T 50% (°C)	Weight lobs (%)	T^2 max (°C)	V^2 max (%/°C)	Weight loss (%)	
PVC	180	280	1.914	285	67	465	0.3169	18.8	12.8
PVC/RMMT(1phr)	181	280	2.128	285.5	70.8	450	0.327	18.8	13.2
PVC/RMMT(2phr)	180	280	1.9780	284	66	460	0.3173	18.8	13.5
PVC/RMMT(3phr)	175	275	2.019	281	68 .8	460	0.3884	18	13
PVC/RMMT(4phr)	175	275	2.023	279.5	68.8	464	0.302	15.8	12.7
PVC/OMMT(1phr)	205	298	0.999	304	63	474	0.2777	16.8	20
PVC/OMMT(2phr)	201	298	1.301	302.8	65.3	473	0.3040	17	17.5
PVC/OMMT(3phr)	199	295	1.619	299.7	66.8	472	0.3124	16.2	16.8
PVC/OMMT(4phr)	196	295	1.7620	299.5	74	468	0.3116	15.8	10

4.6. SEM Study

The SEM was used to study the state of dispersion of nano-Magnetites (modified and unmodified) in the various nanocomposites elaborated. Fig. 16a illustrates the surface morphology of the PVC film, revealing a rough surface characterized by visible irregularities. Additionally, voids can be observed at the interface between the unmelted PVC particles and the PVC matrix. These observations align with results reported by other researchers, who also noted the presence of PVC resin particles smaller than 0.5 µm in size.

They explained that these particles did not completely melt or fuse during the mixing stages [39-42]. Furthermore, the PVC/RMMT nanocomposite films exhibit irregular and non-homogeneous surfaces due to the presence of large RMMT particles on the surface of these films when a low content (1 to 4 phr) of RMMT is incorporated (Fig. 16(b-d)).

Table 3 Light transmission of PVC film and various nanocomposites

Formulation number	MMT Content (phr)	Transmission (%) UV (300 nm)	Visible (550 nm)	IR (900 nm)
PVC	0	46.44	70.21	82.77
PVC/RMMT	1	46.22	64.43	76.43
	2	33.75	52.72	63.19
	3	33.08	54.68	66.74
	4	32.77	49.39	61.26
PVC/OMMT	1	54.83	78.43	98.53
	2	38.86	69.56	82.83
	3	29.93	66.72	84.93
	4	17.98	59.94	81.25

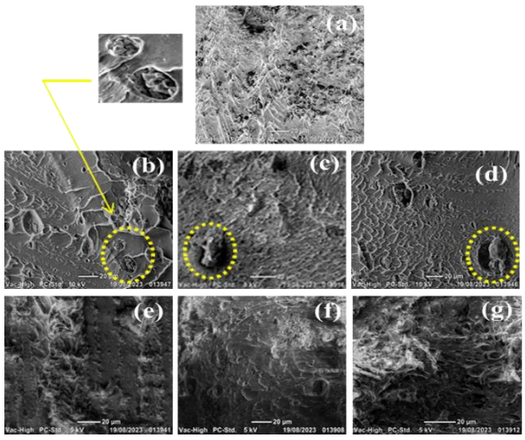

Fig. 16. Microscopy SEM of: (a) film of PVC, (b) PVC/RMMT (1phr), (c) PVC/RMMT (2phr), (d) PVC/RMMT (3phr), (e) PVC/OMM (1phr), (f) PVC/OMMT (2phr), and (g) PVC/OMMT (3phr)

Additionally, the appearance of spheres on the surface of the PVC/RMMT nanocomposite films can be observed, composed of clusters of RMMT particles, indicating RMMT agglomeration (Fig. 16b). This observation suggests an immiscible morphology. On the other hand, organophilic Maghnite (OMMT) disperses uniformly and homogeneously when 1, 2, and 3 phr of OMMT are incorporated into the PVC matrix.

As a result, the surface of the PVC/OMMT nanocomposites becomes less rough compared to the PVC film and the PVC/RMMT nanocomposites (Fig. 16(e-g)).

5. CONCLUSION

Based on all the obtained results, the following conclusions can be drawn: X-ray diffraction (XRD) results show that nanocomposites based on modified Maghnite exhibit an exfoliated structure, while those containing unmodified Maghnite present a microcomposite structure. FTIR spectra confirm the formation of double bonds (C=C) in all the nanocomposites. The addition of OMMT enhances thermal stability due to the nanometric dispersion of fillers in the PVC, limiting the diffusion of heat and volatile decomposition products. Light transmission tests reveal improved transmission in the UV, visible, and IR regions for nanocomposites based on modified Maghnite, attributed to a more uniform particle distribution. Finally, SEM analysis shows more regular surfaces in the nanocomposites based on modified Maghnite, indicating better compatibility with PVC.

REFERENCES

1. *C. M. Chan, J. Wu, J. X. Li, and Y. K. Cheung, "Polypropylene/calcium carbonate nanocomposites," *Polymer*, vol. 43, pp. 2981–2992, 2002, doi: 10.1016/S0032-3861(02)00120-9.*

2. *N. J. Lee and J. Jang, "The effect of fibre content on the mechanical properties of glass fibre mat/polypropylene composites," *Composites Part A*, vol. 30, pp. 815–822, 1999, doi: 10.1016/S1359-835X(98)00185-7.*

3. *N. Othman, H. Ismail, and M. Mariatti, "Effect of compatibilisers on mechanical and thermal properties of bentonite filled polypropylene composites," *Polymer Degradation and Stability*, vol. 91, pp. 1761–1774, 2006, doi: 10.1016/j.polymdegradstab.2005.11.022.*

4. *Y. Kojima, A. Usuki, M. Kawasumi, A. Okada, Y. Fukushima, T. Kurauchi, and O. Kamigaito, "Mechanical properties of nylon 6–clay hybrid," *Journal of Materials Research*, vol. 8, pp. 1185–1189, 1993.*

5. *X. Zhang, "Nanocomposites in tire development – Benefits, challenges, and the role of carbon nanotubes and graphene," *Highlights in Engineering and Technology*, vol. 116, pp. 183–189, 2024, doi: 10.54097/t1dyjv89.*

6. *E. Grosu, "Applications of polyvinylchloride (PVC)/thermoplastic nano-, micro- and macroblends," in *Polyvinylchloride-based Blends: Preparation, Characterization and Applications*, P. M. Visakh and R. N. Darie-Nita, Eds. New York, NY, USA: Springer, 2022, pp. 75–89.*

7. *M. J. M. Acosta, B. F. Tutikian, V. Ortolan, M. L. S. Oliveira, C. H. Sampaio, L. P. Gómez, and L. F. S. Oliveira, "Fire resistance performance of concrete–PVC panels with polyvinyl chloride (PVC) stay-in-place (SIP) formwork," *Journal of Materials Research and Technology*, vol. 8, pp. 4094–4107, 2019, doi: 10.1016/j.jmrt.2019.07.018.*

8. *S. B. A. Boraei, B. Bakhshandeh, F. Mohammadzadeh, D. M. Haghighi, and Z. Mohammadpour, "Clay-reinforced PVC composites and nanocomposites," *Heliyon*, vol. 10, 2024, doi: 10.1016/j.heliyon.2024.e29196.*

9. *F. Kádár, L. Százdi, E. Fekete, and B. Pukánszky, "Surface characteristics of layered silicates: Influence on the properties of clay/polymer nanocomposites," *Langmuir*, vol. 22, pp. 7848–7854, 2006, doi: 10.1021/la060144c.*

10. *B. Belbachir and B. Makhoukhi, "Adsorption of Bezathren dyes onto sodic bentonite from aqueous solutions," *Journal of the Taiwan Institute of Chemical Engineers*, vol. 75, pp. 105–111, 2017, doi: 10.1016/j.jtice.2016.09.042.*

11. *L. Le Pluart, J. Duchet, H. Sautereau, and J. F. Gérard, "Surface modifications of montmorillonite for tailored interfaces in nanocomposites," *Journal of Adhesion*, vol. 78, pp. 645–662, 2002, doi: 10.1080/00218460213738.*

12. *C. K. Bendeddouche, M. Adjdir, and H. Benhaoua, "Stereoselective cyclopropanation under solvent-free conditions catalyzed by a green and efficient recyclable Cu-exchanged bentonite," *Letters in Organic Chemistry*, vol. 13, pp. 217–223, 2016, doi: 10.2174/1570178613666160109005049.*

13. *S. Ayyapan, G. N. Subbanna, R. S. Gopalan, and C. N. R. Rao, "Nanoparticles of nickel and silver produced by the polyol reduction of the metal salts intercalated in montmorillonite," *Solid State Ionics*, vol. 84, pp. 271–281, 1996, doi: 10.1016/0167-2738(96)00021-5.*

14. *C. H. Chen, C. H. Teng, M. Tsai, and F. Yen, "Preparation and characterization of rigid poly(vinyl chloride)/MMT nanocomposites. II. XRD, morphological and mechanical characteristics," *Journal of Polymer Science Part B: Polymer Physics*, vol. 44, pp. 2145–2154, 2006, doi: 10.1002/polb.20880.*

15. *W. Xu, Z. Zhou, M. Ge, and W. P. Pan, "Poly(vinyl chloride)/montmorillonite nanocomposites: Glass transition temperature and mechanical properties," *Journal of Thermal Analysis and Calorimetry*, vol. 78, pp. 91–99, 2004, doi: 10.1023/B:JTAN.0000042157.96074.44.*

16. *F. Bouzidi, M. Guessoum, M. Fois, and N. Haddaoui, "Viscoelastic, thermo-mechanical and environmental properties of composites based on polypropylene/poly(lactic acid) blend and copper-modified nanoclay," *Journal of Adhesion Science and Technology*, vol. 32, pp. 496–515, 2018, doi: 10.1080/01694243.2017.1365422.*

17. *M. B. Ahmad, W. H. Hoidy, B. I. Nor Azowa, and E. A. J. Al-Mulla, "Modification of montmorillonite by new surfactants," *Journal of Engineering and Applied Sciences*, vol. 4, pp. 184–188, 2009.*

18. *D. Dai and M. Fan, "Investigation of the dislocation of natural fibres by Fourier transform infrared spectroscopy," *Vibrational Spectroscopy*, vol. 55, pp. 300–306, 2011, doi: 10.1016/j.vibspec.2010.12.009.*

19. *S. Bouhank and S. Nekkaa, "Effects of chemical treatments on the structural, mechanical and morphological properties of poly(vinyl chloride)/Spartium junceum fiber composites," *Cellulose Chemistry and Technology*, vol. 49, pp. 375–385, 2015.*

20. *D. E. Kheeoub, M. Belbachir, and S. Lamouri, "Nylon 6/clay nanocomposites prepared with Algerian modified clay (12-maghnite)," *Reviews in Chemical Engineering*, vol. 41, pp. 5217–5228, 2015, doi: 10.1007/s11164-014-1623-8.*

21. *C. Wan, Y. Zhang, and Y. Zhang, "Effect of alkyl quaternary ammonium on processing discoloration of melt-intercalated PVC–montmorillonite composites," *Polymer Testing*, vol. 23, pp. 299–306, 2004, doi: 10.1016/j.polymertesting.2003.08.001.*

22. *J. Pagacz and K. Pielichowski, "Preparation and characterization of PVC/montmorillonite nanocomposites: A review," *Journal of Vinyl and Additive Technology*, vol. 15, pp. 61–76, 2009, doi: 10.1002/vnl.20186.*

23. *H. Andreas, *Plastics Additives Handbook*. USA: Hanser Publishers, 1993.*

24. *F. Gong, M. Feng, G. Zhao, S. Zhang, and M. Yang, "Thermal properties of poly(vinyl chloride)/montmorillonite nanocomposites," *Polymer Degradation and Stability*, vol. 84, pp. 289–294, 2004, doi: 10.1016/j.polymdegradstab.2003.11.003.*

25. *K. C. Mensker and G. T. Fedoseeva, *The Degradation and Stabilization of PVC*. New York, NY, USA: Chemistry Press, 1979.*

26. *G. Scott and M. Tahan, "Effect of some additives on the photoxidation of rigid PVC," *European Polymer Journal*, vol. 11, pp. 535–539, 1975, doi: 10.1016/0014-3057(75)90106-8.*

27. *G. Scott, M. Tahan, and J. Vyvoda, "The effect of thermal processing on PVC—III. Photo-oxidation of unstabilized PVC," *European Polymer Journal*, vol. 14, pp. 1021–1026, 1978, doi: 10.1016/0014-3057(78)90161-1.*

28. *T. Marconi, T. Faravelli, G. Bozzano, M. Dente, and E. Ranzi, "Thermal degradation of poly(vinyl chloride)," *Journal of Analytical and Applied Pyrolysis*, vol. 70, pp. 519–553, 2003, doi: 10.1016/S0165-2370(03)00024-X.*

29. *J. C. Garcia-Quesada, A. Marcilla, and M. Gilbert, "Thermal degradation of silane crosslinked unplasticized PVC," *Journal of Analytical and Applied Pyrolysis*, vol. 60, pp. 159–177, 2001, doi: 10.1016/S0165-2370(00)00190-X.*

30. *T. Peprnicek, J. Duchet, L. Kovarova, J. Malac, J. F. Gérard, and J. Simonik, "Poly(vinyl chloride)/clay nanocomposites: X-ray diffraction, thermal and rheological behavior," *Polymer Degradation and Stability*, vol. 91, pp. 1855–1860, 2006, doi: 10.1016/j.polymdegradstab.2005.11.003.*

31. *C. Wan, X. Qiao, Y. Zhang, and X. Zhang, "Effect of different clay treatment on morphology and mechanical*

*properties of PVC–clay nanocomposites," *Polymer Testing*, vol. 22, pp. 453–463, 2003, doi: 10.1016/S0142-9418(02)00126-5.*

32. *N. Karakehya and S. Bilgic, "Surface characterization of montmorillonite/PVC nanocomposites by inverse gas chromatography," *International Journal of Adhesion and Adhesives*, vol. 51, pp. 140–147, 2014, doi: 10.1016/j.ijadhadh.2014.03.001.*

33. *B. Bouchoul, M. T. Benaniba, and V. Massardier, "Effect of biobased plasticizers on thermal, mechanical, and permanence properties of poly(vinyl chloride)," *Journal of Vinyl and Additive Technology*, vol. 20, pp. 260–267, 2014, doi: 10.1002/vnl.21356.*

34. *P. Jia, C. Bo, L. Hu, M. Zhang, and Y. Zhou, "Synthesis of a novel polyester plasticizer based on glyceryl monooleate and its application in poly(vinyl chloride)," *Journal of Vinyl and Additive Technology*, vol. 22, pp. 514–519, 2016, doi: 10.1002/vnl.21468.*

35. *Y. Yang, J. Huang, R. Zhang, and J. Zhu, "Designing bio-based plasticizers: Effect of alkyl chain length on plasticization properties of isosorbide diesters in PVC blends," *Materials & Design*, vol. 126, pp. 29–36, 2017, doi: 10.1016/j.matdes.2017.04.005.*

36. *T. Abdel-Baset, M. Elzayat, and S. Mahrou, "Characterization and optical and dielectric properties of polyvinyl chloride/silica nanocomposites films," *International Journal of Polymer Science*, vol. 2016, pp. 1–13, 2016, doi: 10.1155/2016/1707018.*

37. *A. M. El Sayed, S. El-Sayed, W. M. Morsi, S. Mahrous, and A. Hassen, "Synthesis, characterization, optical, and dielectric properties of polyvinyl chloride/cadmium oxide nanocomposite films," *Polymer Composites*, vol. 35, pp. 1842–1851, 2014, doi: 10.1002/pc.22839.*

38. *B. Bouchoul and M. T. Benaniba, "Assessment of derived sunflower oil as environmentally friendly plasticizers in poly(vinyl chloride)," *Polímeros*, vol. 31, pp. 1–9, 2021, doi: 10.1590/0104-1428.20210015.*

39. *T. Ren, J. Yang, Y. Huang, J. Ren, and Y. Liu, "Preparation, characterization, and properties of poly(vinyl chloride)/compatibilizer/organophilic-montmorillonite nanocomposites," *Polymer Composites*, vol. 27, pp. 55–64, 2006, doi: 10.1002/pc.20161.*

40. *Y. Hamid, A. Aznizam, and N. Deirram, "Mechanical and morphological properties of waste *Eurycoma longifolia* fiber/montmorillonite reinforced poly(vinyl chloride) hybrid composites," *Journal of Applied Polymer Science*, vol. 128, pp. 1170–1175, 2013, doi: 10.1002/app.38401.*

41. *D. Wu, X. Wang, Y. Song, and R. Jin, "Nanocomposites of poly(vinyl chloride) and nanometric calcium carbonate particles: Effects of chlorinated polyethylene on mechanical properties, morphology, and rheology," *Journal of Applied Polymer Science*, vol. 92, pp. 2714–2723, 2004, doi: 10.1002/app.20295.*

42. *C. H. Chen, R. D. Wesson, J. R. Collier, and Y. W. Lo, "Studies of rigid poly(vinyl chloride) compounds. I. Morphological characteristics of poly(vinyl chloride)/chlorinated polyethylene blends," *Journal of Applied Polymer Science*, vol. 58, pp. 1087–1091, 1995, doi: 10.1002/app.1995.070580701*